



LAWRENCE
LIVERMORE
NATIONAL
LABORATORY

Effects of Heat Conduction on Artificial Viscosity Methods for Shock Capturing

A. W. Cook

December 17, 2012

Journal of Computational Physics

Disclaimer

This document was prepared as an account of work sponsored by an agency of the United States government. Neither the United States government nor Lawrence Livermore National Security, LLC, nor any of their employees makes any warranty, expressed or implied, or assumes any legal liability or responsibility for the accuracy, completeness, or usefulness of any information, apparatus, product, or process disclosed, or represents that its use would not infringe privately owned rights. Reference herein to any specific commercial product, process, or service by trade name, trademark, manufacturer, or otherwise does not necessarily constitute or imply its endorsement, recommendation, or favoring by the United States government or Lawrence Livermore National Security, LLC. The views and opinions of authors expressed herein do not necessarily state or reflect those of the United States government or Lawrence Livermore National Security, LLC, and shall not be used for advertising or product endorsement purposes.

Effects of Heat Conduction on Artificial Viscosity Methods for Shock Capturing

Andrew W. Cook

Lawrence Livermore National Laboratory, Livermore, CA 94551, USA

Abstract

We investigate the efficacy of artificial thermal conductivity for shock capturing. The conductivity model is derived from artificial bulk and shear viscosities, such that stagnation enthalpy remains constant across shocks. By thus fixing the Prandtl number, more physical shock profiles are obtained, only on a larger scale. The conductivity model does not contain any empirical constants. It increases the net dissipation of a computational algorithm but is found to better preserve symmetry and produce more robust solutions for strong-shock problems.

Keywords: Large-Eddy Simulation, subgrid-scale models, shocks, turbulence, artificial viscosity, thermal conductivity, stagnation enthalpy

Artificial viscosities have been employed for over six decades to capture shocks in high Mach number flows [1]. By incorporating viscous terms in the momentum and energy equations, shocks can be spread over several grid points, thus regularizing solutions on discrete meshes. At the molecular scale, shocks have internal structure, which depends not only on the viscosity but also on the thermal conductivity of the fluid. Typical Prandtl numbers for air and many other gases near atmospheric conditions are on the order of unity. However, in numerical simulations employing artificial viscosity, thermal conductivity is often neglected, or else employed in a manner unrelated to viscosity, such that the *effective* Prandtl number inside shocks is much greater than unity. This can have unintended consequences, such as “wall heating” [2, 3]. The purpose of this Short Note is to explore the pros and cons of an artificial conductivity that mimics the relationship of physical conductivity to physical viscosity. The artificial conductivity is designed to produce numerical shock profiles similar to physical shock profiles, but rescaled from

the molecular realm to the grid scale.

For simplicity, consider a one-dimensional shock in a coordinate system in which the shock is stationary. The steady-state conservation equations can be spatially integrated to yield:

$$\rho u = \rho_1 u_1 , \quad (1)$$

$$p + \rho u^2 - \tau_{xx} = p_1 + \rho_1 u_1^2 , \quad (2)$$

$$\rho u(h + u^2/2) + q_x - u\tau_{xx} = \rho_1 u_1(h_1 + u_1^2/2) , \quad (3)$$

where ρ is density, u is velocity, p is pressure, h is enthalpy, τ_{xx} is viscous stress, q_x is heat conduction and the 1 subscripts denote upstream supersonic conditions. The enthalpy is

$$h = e + p/\rho = c_p T \quad (4)$$

where e is thermal energy, T is temperature and c_p is constant-pressure specific heat. Equations (1), (2) and (3) apply locally within the shock wave. The Rankine-Hugoniot jump conditions require the stagnation enthalpy to match on either side of the shock; i.e.,

$$h_2 + u_2^2/2 = h_1 + u_1^2/2 , \quad (5)$$

where the 2 subscripts denote downstream subsonic conditions. Comparison of (3) and (5) suggests that a useful form of artificial conductivity can be deduced by requiring the stagnation enthalpy, $h + u^2/2$, to be constant inside the shock as well as on either side. This is equivalent to enforcing

$$\frac{dh}{dx} + u \frac{du}{dx} = 0 \quad (6)$$

throughout the shock wave. The Fourier heat flux then becomes

$$q_x \equiv -\kappa \frac{dT}{dx} = -\frac{\kappa}{c_p} \frac{dh}{dx} = \frac{\kappa}{c_p} u \frac{du}{dx} , \quad (7)$$

where κ is thermal conductivity. The Navier-Stokes viscous stress is

$$\tau_{xx} \equiv \left(\beta + \frac{4}{3}\mu \right) \frac{du}{dx} , \quad (8)$$

where β is bulk viscosity and μ is shear viscosity. We see from (3) that a constant stagnation enthalpy requires $q_x = u\tau_{xx}$ or $k/c_p = (\beta + 4\mu/3)$. Hence, a promising conductivity model for preserving monotonicity across the shock is

$$\kappa = (\beta + 4\mu/3) h/T . \quad (9)$$

A convenient feature of this model is that it does not involve any empirical constants. Note that for $\beta = 0$, (9) is equivalent to setting the Prandtl number to $3/4$ [4]. Lee et al. [5] successfully employed (9) (with $\beta = 0$ and a temperature-dependent μ) in their Direct Numerical Simulations of a shock interacting with isotropic turbulence. Here we explore the efficacy of (9) for Large-Eddy Simulations (LES), wherein subgrid-scale models may be employed for μ and/or β .

For the simulations reported herein, we employ the following grid-dependent viscosity models [6, 7, 8, 9, 10]:

$$\mu = 0.002\rho |\nabla^4 (SL^6)| , \quad (10)$$

$$\beta = \rho |\nabla^4 (\nabla \cdot \mathbf{u})| L^6 H(-\nabla \cdot \mathbf{u}) , \quad (11)$$

where S is the magnitude of the strain-rate tensor, L is the grid spacing, H is the Heaviside function, ∇^4 is the biharmonic operator and the overbar $(\overline{})$ denotes a gaussian filter of width $4L$. The factor of 0.002 in (10) was empirically determined to produce the correct subgrid energy flux for decaying turbulence [7] and the Taylor-Green vortex [8]. The Navier-Stokes equations are solved in strong conservation form with spatial derivatives computed via tenth-order compact differencing [11] and temporal integration accomplished via fourth-order Runge-Kutta timestepping [12]. Since the compact stencils are purely centered, there is zero numerical dissipation associated with the spatial differencing algorithm. The explicit Runge-Kutta time-stepping scheme introduces only very slight dissipation [6]. The role of μ and β in LES is to keep the solution smooth at the grid scale in order to avoid Gibbs phenomenon and other ringing associated with flow discontinuities.

As a first test of the conductivity model (9), we consider the spherical Noh implosion [2]. The nondimensional initial conditions are: $\rho = 1$, $p = 0$ and $\mathbf{u} =$ unit vector directed toward origin, with an adiabatic index of $\gamma = 5/3$ (all test problems herein use an ideal-gas equation of state). In this problem, an infinite-strength shock expands outward from the origin at a constant radial velocity of $1/3$. In Figure 1, the results of simulations with

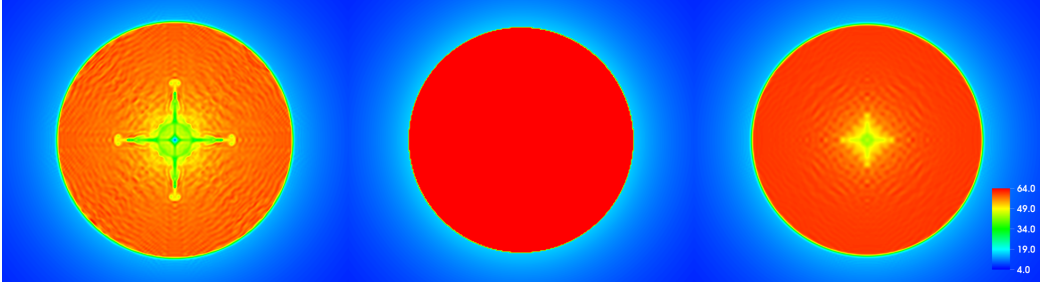


Figure 1: Density at $t = 0.6$ for the spherical Noh implosion. The shock at this time should be located at a radius of 0.2. The simulations were performed on a uniform Cartesian grid with spacing $L = 0.002$. The simulation on the left is without conductivity, the simulation on the right is with conductivity and the plot in the center is the exact solution.

and without thermal conductivity are compared to the exact solution. The artificial thermal conductivity is here seen to reduce wall heating and produce a shock slightly closer to the exact location. The conductivity model also reduces spurious oscillations behind the shock and helps preserve spherical symmetry.

As a second test of the artificial conductivity, we consider the spherical Sedov-Taylor-von Neumann blast wave [13, 14, 15]. Whereas the Noh problem is purely compressive, the Sedov blast wave is strongly expansive. The initial/flow conditions are: $\rho = 1$, $\mathbf{u} = 0$, $e = 0.8510718547582291\delta(r)$ and $\gamma = 1.4$. With this initial energy source, the shock propagates outward to a radius of $r = 1$ at $t = 1$. A challenging aspect of this problem is the near vacuum left behind at the origin. For a momentum-conserving solver, the low density near the origin magnifies errors in the velocity field. Computed velocity fields, with and without conduction, are compared to the exact solution in Figure 2. Once again, the artificial conductivity helps preserve spherical symmetry and produces a flow closer to the exact solution.

As a third test, we consider the slowly moving shock studied by Jin and Liu [16]. The initial conditions are: $\rho = 3.86$, $u = -0.81$, $e = 6.690421502590674$ for $x < 0.5$ and $\rho = 1.0$, $u = -3.44$, $e = 2.5$ for $x \geq 0.5$, with $\gamma = 1.4$. These conditions result in a Mach-3 shock traveling to the right with speed 0.1096. Figure 3 shows momentum at $t = 1.0$. Jin and Liu [16] have shown that upwind schemes applied to this problem generate large momentum spikes ahead of the shock and exhibit strong oscillations behind the shock. The momentum spike is caused by numerical viscosity introduced into the continuity equation by upwinding. The present (centered) scheme does not generate

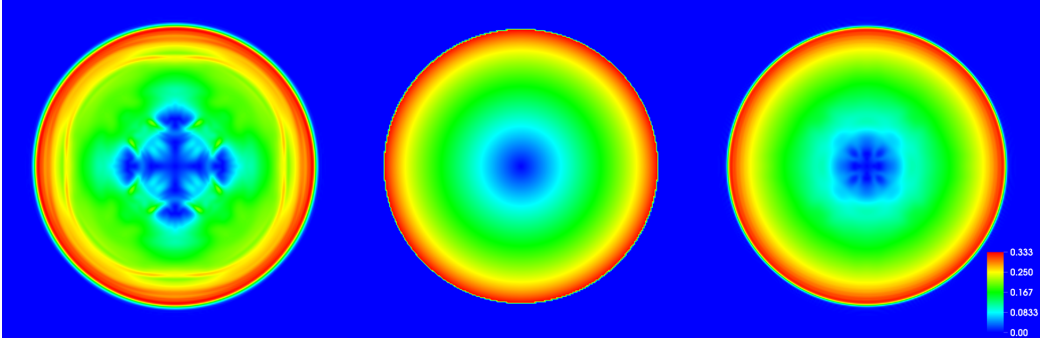


Figure 2: Velocity magnitude at $t = 1.0$ for the spherical Sedov blast wave. The simulations were conducted on a uniform Cartesian grid with spacing $L = 0.01$. The simulation on the left is without conductivity, the simulation on the right is with conductivity and the plot in the center is the exact solution.

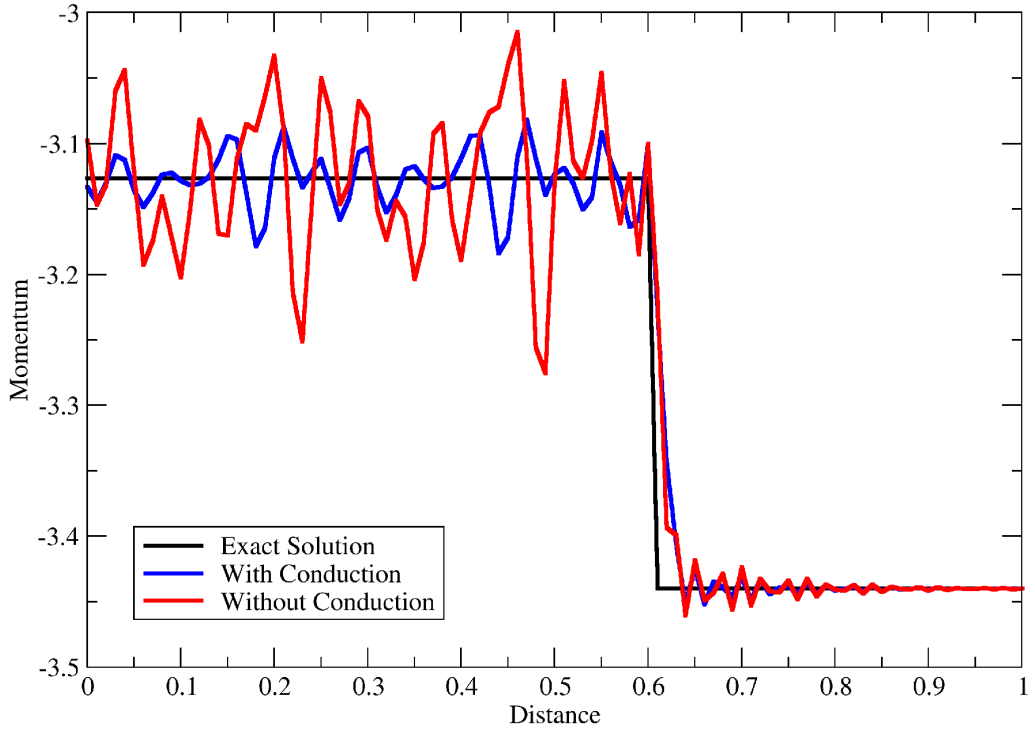


Figure 3: Momentum (ρu) at $t = 1.0$ for Jin-Liu shock, using a grid spacing of $L = 0.01$.

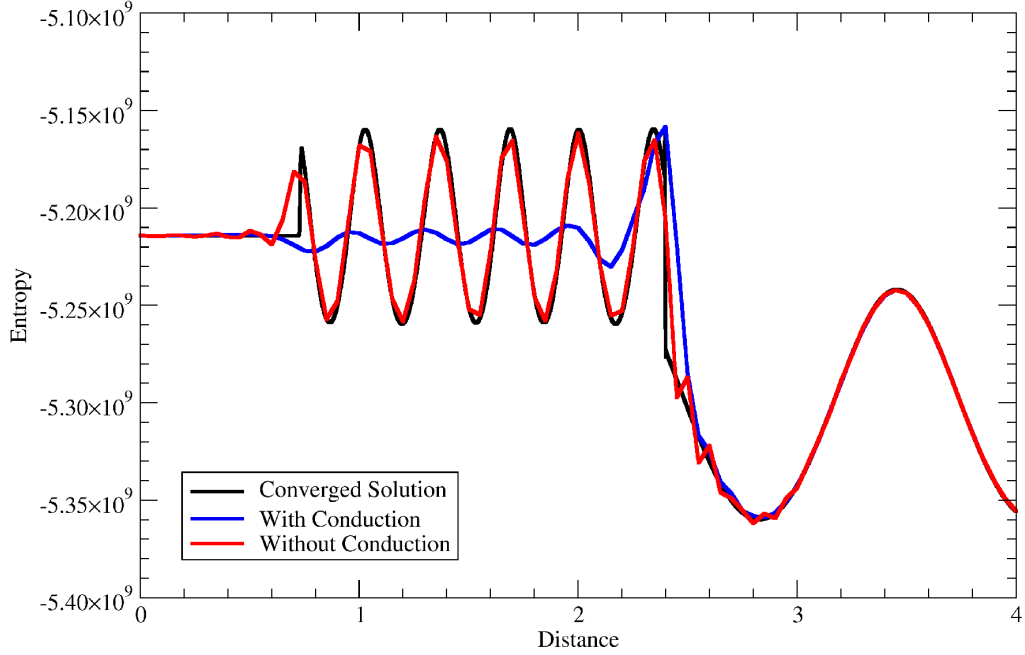


Figure 4: Entropy at $t = 1.8$ for Shu's problem using $L = 0.05$.

the anomalous momentum spike but still suffers from oscillations generated by the unsteadiness of the discrete shock profile. The conductivity model reduces the spurious oscillations by half, both ahead and behind the shock. Artificial conduction significantly improves the solution in this case, although it does not completely solve the problem.

Our fourth test is the Shu-Osher problem, a canonical model of a one-dimensional shock-turbulence interaction [17]. The initial conditions are: $\rho = 3.857143$, $p = 10.333333$, $u = 2.629369$ for $x < -4$ and $\rho = 1 + 0.2 \sin(5x)$, $p = 1$, $u = 0$ for $x \geq -4$, with $\gamma = 1.4$. As the shock propagates into the sinusoidal density field, it leaves a steeply oscillating flow in the post-shock region. Figure 4 shows the entropy solution at $t = 1.8$. In this case, artificial conduction fortunately removes the unphysical pre-shock oscillations but unfortunately damps the physical post-shock oscillations. Entropy behind the shock is very sensitive to heat conduction. With the conduction model turned on, a grid resolution of $L = 0.01$ is required to match the amplitude of the post-shock oscillations of the case with the model off. The problem here is that the wavelength of the post-shock oscillations is too close

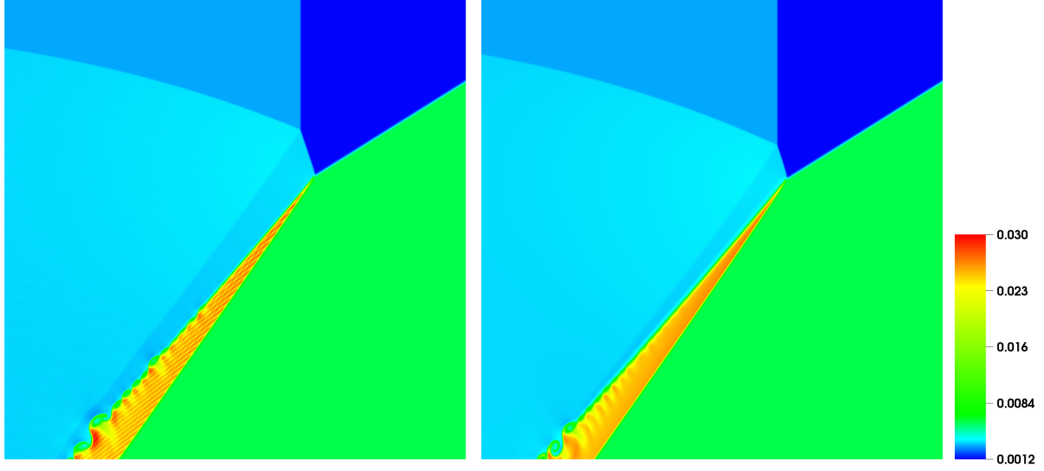


Figure 5: Density at $t = 10 \mu\text{s}$ for shock impacting an air-SF6 interface. The simulations were conducted on a uniform Cartesian grid with $L = 2 \mu\text{m}$.

to the grid scale for the model to distinguish between physical and numerical ringing. With the conduction model active, the grid must be refined until a separation of scales is achieved.

Our fifth and final test is the fast-slow gas interface experiment of Abd-El-Fattah and Henderson [18]. In one series of experiments, an incident shock, traveling in air with a pressure jump of 4, impacts an inclined SF6 interface. The shock lays down a vortex sheet at the interface and the interaction generates an irregular refraction at the triple point. An interesting feature of this interaction is the formation of a Mach stem. In numerical simulations, the length of the Mach stem is known to be sensitive to grid resolution and the amount of dissipation in the computational algorithm. We initialize our simulations with the interface at an angle of 58 degrees with respect to a Mach 1.89 shock. The pre-shocked air and SF6 are at a pressure of 1 bar and temperature of 295 K. At $t = 0$ the shock is located 1 mm away from the closest edge of the SF6 interface. Figure 5 shows the density field at $t = 10 \mu\text{s}$. The shocked interface is Kelvin-Helmholtz unstable due to the difference in shock speed for the two gases. Grid-seeded perturbations thus grow into an array of vortices along the interface. In the case with no conduction, grid-perturbations to the discrete shock profile generate pressure waves, which propagate across the triangular region of the shocked SF6 (see left image in Fig. 5). With the conduction model turned on, the discrete shock profile

is more monotonic and the anomalous pressure waves never get generated. The improved solution in the shocked SF6 region comes at the expense of a reduced Mach stem, which is a result of the extra dissipation introduced by the artificial heat conduction.

From the results of these test problems, we may draw several conclusions regarding the fixed-Prandtl-number conductivity model. Some significant advantages are: (A) more physical shock profiles, albeit at a larger scale; (B) alleviation of wall heating; (C) symmetry preservation, e.g., spherical implosions/explosions on square grids; (D) reduction of spurious oscillations around shocks and (E) removal of grid-seeded pressure waves. The primary disadvantages of the model are: (A) increased damping of small-scale physical oscillations and (B) dissipation of features that are sensitive to sharp entropy and/or energy gradients. In summary, experience with the current solver has shown that the best results are achieved by employing the conduction model with sufficient grid resolution, such that features of interest are well resolved. The computational cost of the model is negligible and it is extremely simple to implement; hence, it ought to prove useful in almost any LES code employing artificial or subgrid-scale viscosity.

Acknowledgements

This work was performed under the auspices of the U.S. Department of Energy by Lawrence Livermore National Laboratory under Contract DE-AC52-07NA27344.

- [1] J. von Neumann, R. D. Richtmyer, A method for the numerical calculations of hydrodynamical shocks, *J. Appl. Phys.* 21 (1950) 232–237.
- [2] W. F. Noh, Errors for calculations of strong shocks using an artificial viscosity and an artificial heat flux, *J. Comput. Phys.* 72 (1987) 78–120.
- [3] W. J. Rider, Revisiting wall heating, *J. Comput. Phys.* 162 (2000) 395–410.
- [4] W. G. Vincenti, C. H. J. Kruger, Robert E. Drieger Publishing Company, Malabar, Florida, pp. 412–416.
- [5] S. Lee, S. K. Lele, P. Moin, Direct numerical simulation of isotropic turbulence interacting with a weak shock wave, *J. Fluid Mech.* 251 (1993) 533–562.
- [6] A. W. Cook, W. H. Cabot, A high-wavenumber viscosity for high-resolution numerical methods, *J. Comput. Phys.* 195 (2004) 594–601.
- [7] A. W. Cook, W. H. Cabot, Hyperviscosity for shock-turbulence interactions, *J. Comput. Phys.* 203 (2005) 379–385.
- [8] A. W. Cook, Artificial fluid properties for large-eddy simulation of compressible turbulent mixing, *Phys. Fluids* 19 (2007) 055103.
- [9] A. W. Cook, Enthalpy diffusion in multicomponent flows, *Phys. Fluids* 21 (2009) 055109.
- [10] A. W. Cook, M. S. Ulitsky, D. S. Miller, Hyperviscosity for unstructured ALE meshes, *Int. J. Comput. Fluid Dyn.* in press (2012).
- [11] S. K. Lele, Compact finite difference schemes with spectral-like resolution, *J. Comput. Phys.* 103 (1992) 16–42.
- [12] C. A. Kennedy, M. H. Carpenter, R. M. Lewis, Low-storage, explicit Runge-Kutta schemes for the compressible Navier-Stokes equations, *Applied Numerical Mathematics* 35 (2000) 177–219.

- [13] L. I. Sedov, Similarity and Dimensional methods in Mechanics, Fourth Ed., Academic Press, New York, 1959.
- [14] G. I. Taylor, The formation of a blast wave by a very intense explosion: I, ii, Proc. Roy. Soc. London, Ser. A 201 (1950) 155–175.
- [15] L. D. Landau, E. M. Lifshitz, Fluid Mechanics, Addison-Wesley, Reading, Mass., 1959.
- [16] S. Jin, J.-G. Liu, The effects of numerical viscosities I. Slowly moving shocks, J. Comput. Phys. 126 (1996) 373–389.
- [17] C.-W. Shu, S. J. Osher, Efficient implementation of essentially non-oscillatory shock capturing schemes II, J. Comput. Phys. 83 (1989) 32–78.
- [18] A. M. Abd-El-Fattah, L. F. Henderson, Shock waves at a fast-slow gas interface, J. Fluid Mech. 86 (1978) 15–32.